American Mineralogist, Volume 61, pages 229–237, 1976

Crystal chemistry of the serandite—pectolite series and related minerals

YOSHIO TAKÉUCHI, YASUHIRO KUDOH AND TAKAMITSU YAMANAKA

Mineralogical Institute, Faculty of Science, University of Tokyo
Hongo, Tokyo 113, Japan

Abstract

The serandite structure has been refined to $R = 3.0$ percent, using a crystal from Tanohata mine, Japan (approximately 39.9°N, 141.9°E), $P\bar{1}$, a 7.683(1), b 6.889(1), c 6.747(1) Å, α 90.53(5)°, β 94.12(2)°, γ 102.75(2)°, $Z = 2 \times [(Mn_{1.88}Ca_{0.17}Mg_{0.01})Na_{1.00}HSi_{2.97}O_9]$. The noteworthy features of the structure of serandite which is isotypic to pectolite include: (1) Almost all Si–O and all Na–O lengths are smaller than the corresponding lengths in pectolite; the mean values are 1.623(2)[1.630(2)] Å and 2.485(1)[2.580(1)] Å respectively (values in brackets are those for pectolite). (2) A comparison of the serandite and pectolite structures suggests that the shrinkage of octahedral bands due to substitution of Mn for Ca gives rise to distortions of individual silicate tetrahedra rather than a change in configuration of silicate chains. (3) Ca atoms are preferably located at the $M(1)$ position which corresponds to Ca(1) in the pectolite structure; the occupany at $M(1)$ is 0.84(1) Mn and 0.16(1)Ca.

The specific mode of cation ordering has been interpreted based on the following geometrical considerations: (1) the relations between the configuration of Si_3O_9 chains and the size of cation octahedra; and (2) the location of silicate chains relative to octahedral bands. Rules brought out from these considerations may be used to explain the modes of cation ordering in the wollastonite-group minerals in general.

Introduction

The pectolite ($Ca_2NaHSi_3O_9$)–serandite ($Mn_2NaHSi_3O_9$) series is of particular interest because it provides a rare example of solid solution in silicate minerals where the substitution of Mn for Ca extends over the whole range of the series while the structure type remains unchanged (Schaller, 1955). None of the structures of minerals in this series have been investigated except that of pectolite, which was determined by Buerger (1956) and refined by Prewitt and Buerger (1963) and further by Prewitt (1967). We have therefore carried out a structural study of serandite to elucidate the crystal chemical nature of the series. That part of the study concerning the procedure of structure analysis has been reported separately (Takéuchi *et al.*, 1973) as an example of application of the partial Patterson method (Takéuchi, 1972a). A brief account on the hydrogen-bonded system of serandite has also appeared (Takéuchi and Kudoh, 1972). The present paper reports the details of the structure and offers a crystal chemical discussion on the pectolite–serandite series and related minerals such as wollastonite and bustamite. Though crystal chemical aspects of the wollastonite group minerals were discussed by Prewitt and Buerger (1963), Peacor and Prewitt (1963), and by Prewitt and Peacor (1964), a different approach is provided in the present paper.

Experimental

Well developed serandite crystals (up to 10 cm long and several cm wide on cleaved faces) from the Tanohata mine were used in the present study. Electron microprobe analyses (Table 1) revealed that the chemical composition of the specimens was close to that of the Mn end-member of the serandite–pectolite series, giving a formula of:

$$(Mn_{1.88}Ca_{0.17}Mg_{0.01})Na_{1.00}HSi_{2.97}O_9.$$

The cell dimensions, which were determined with a four-circle diffractometer (Mo$K\alpha$ = 0.70926 Å), are compared in Table 2 with those of pectolite (Prewitt, 1967). The unit cell contains two of the above chemical units. Space group $P\bar{1}$ was assumed on the basis of the triclinic diffraction symmetry and the results of an $N(z)$ test (Howells *et al.*, 1950) which showed the existence of a center of symmetry.

TABLE 1. Microprobe analyses*

		Number of atoms calculated for 17 oxygen atoms**
Na_2O	8.63 wt. %	1.99
MnO	37.33	3.76
CaO	2.62	0.33
MgO	0.13	0.02
FeO	0.13	0.01
K_2O	0.01	0.00
Al_2O_3	-	-
TiO_2	-	-
SiO_2	49.88	5.94
Total	98.73**	

* An average of analyses of five different positions of a crystal.
** Excluding H_2O.

The crystal used for intensity measurements is elongated parallel to the *b* axis, with a length of 0.32 mm. It is bounded by the (101) and ($\bar{1}$01) cleavages; the dimensions of the cross section were 0.063 × 0.088 mm². The ω-2θ scan technique was used to measure a total of 2043 reflections to sin $\theta/\lambda = 0.70$ (Mo$K\alpha$). Of these, 1766 reflections which have intensities greater than $2\sigma(I)$ were used for the structure refinement. After correcting for Lorentz and polarization factors, the intensities were reduced to structure factors. No corrections were made for absorption (μ = 42.9 cm^{-1}) and secondary extinction.

Refinement of the structure

As described elsewhere (Takéuchi *et al.*, 1973), the approximate atomic coordinates that gave an R = 0.35 were derived with the use of the partial Patterson method (Takéuchi, 1972a). The atomic coordinates and isotropic thermal parameters were then refined using the full-matrix least-squares program, ORFLS (Busing *et al.*, 1962). The atomic form factors were provided by Volume III of the *International Tables for X-ray Crystallography*. The nonionized state was used for Si and O. Several cycles of calculations applying unit weight readily reduced to initial R value to 0.042.

At this stage of the refinement, inspection of calculated and observed structure factors revealed that 50 reflections were apparently affected by secondary extinction. An anisotropic refinement excluding these reflections converged to give an R = 0.034. A weighting factor was used of the form (Cruickshank, 1965):

$$w = 1/(a + F_o + cF_o^2),$$

where a = 10.0 and c = 0.01.

The difference Fourier map subsequently prepared revealed a significant negative peak at one of the two sets of Mn positions. Noting that our structure contained 0.34 Ca per cell, we suspected that the negative peak might be due to the substitution of Ca at this position. We therefore continued the least-square refinement introducing occupancy parameters to the two Mn positions following the procedure of Finger (1969); total content of Mn and Ca per cell was constrained to agree with the chemical composition of our crystals. The calculations converged at an R value of 0.030. The maximum and mean shifts of atomic coordinates, as a fraction of σ in the final cycle of calculation, were respectively 0.22 and 0.06. The site refinement showed that Ca was concentrated at one of the Mn positions, denoted $M(1)$.The site contents determined are given in Table 3. The $M(1)$ and $M(2)$ sites correspond, respectively, to Ca(1) and Ca(2) of the pectolite structure (Prewitt, 1967). In Table 3, the final atomic coordinates and isotropic temperature factors are compared with those of pectolite (Prewitt, 1967). The anisotropic thermal parameters are given in Table 4, and observed and calculated structure factors in Table 5.[1]

[1] To obtain a copy of this table, order Document Am-76-019 from the Business Office, Mineralogical Society of America, 1909 K Street, N.W., Washington, D.C. 20006. Please remit $1.00 in advance for the microfiche.

TABLE 2. Comparison of cell dimensions between serandite and pectolite

	a	b	c	α	β	γ	Space group
serandite	7.683(1) Å	6.889(1) Å	6.747(1) Å	90.53(5)°	94.12(2)°	102.75(2)°	$P\bar{1}$
pectolite (Prewitt, 1967)	7.988	7.040	7.025	90.52	95.18	102.47	$P\bar{1}$

Numbers in parentheses represent standard errors.

TABLE 3. Atomic coordinate and isotropic temperature factors of serandite and pectolite

Atom	Site content	x	y	z	B
M(1)	0.84 Mn, 0.16 Ca	0.8527(1)	0.5943(1)	0.1363(1)	0.54 Å^2
	1.0 Ca	0.8548	0.5936	0.1449	0.41
M(2)	0.98 Mn, 0.02 Ca	0.8497(1)	0.0840(1)	0.1332(1)	0.45
	1.0 Ca	0.8467	0.0839	0.1405	0.39
Na		0.5574(2)	0.2548(2)	0.3518(2)	1.18
		0.5524	0.2596	0.3433	1.16
Si(1)		0.2166(1)	0.4025(1)	0.3414(1)	0.34
		0.2185	0.4015	0.3374	0.21
Si(2)		0.2071(1)	0.9527(1)	0.3506(1)	0.33
		0.2150	0.9544	0.3440	0.22
Si(3)		0.4546(1)	0.7389(1)	0.1429(1)	0.33
		0.4505	0.7353	0.1447	0.19
O(1)		0.6643(3)	0.7953(4)	0.1146(4)	0.68
		0.6526	0.7871	0.1280	0.35
O(2)		0.3235(3)	0.7079(4)	-0.0568(3)	0.65
		0.3300	0.7043	-0.0535	0.31
O(3)		0.1809(3)	0.4952(3)	0.5534(4)	0.79
		0.1864	0.4960	0.5395	0.34
O(4)		0.1599(3)	0.8458(3)	0.5568(4)	0.78
		0.1783	0.8465	0.5411	0.44
O(5)		0.0611(3)	0.3908(4)	0.1683(3)	0.61
		0.0633	0.3860	0.1733	0.34
O(6)		0.0531(3)	0.8930(4)	0.1727(3)	0.65
		0.0600	0.8961	0.1768	0.34
O(7)		0.4077(3)	0.5331(3)	0.2739(4)	0.65
		0.3992	0.5349	0.2720	0.36
O(8)		0.3974(3)	0.9052(3)	0.2880(4)	0.66
		0.3955	0.9092	0.2746	0.39
O(9)		0.2614(3)	0.1899(3)	0.3928(3)	0.69
		0.2628	0.1908	0.3851	0.32

The values for serandite are given in the first line of each pair, and those for pectolite (Prewitt, 1967) in the second. Errors in atomic coordinates of pectolite are 0.0001 for Ca, 0.0002 for Na, and 0.0004 for O. The B's are equivalent isotropic values (Hamilton, 1959). Calculated standard errors in site content of serandite are 0.007.

Discussion of the structure

Figure 1 shows the serandite structure projected onto (101). Mn octahedra share edges to form bands, two octahedra wide, parallel to the *b* axis. Each Na atom has six near oxygen atoms, within a distance of 2.6 Å, and two additional oxygen neighbours, at a distance of approximately 3.0 Å, that form a distorted square antiprism which is similar to the polyhedron about Ca in the structure of johannsenite (Freed and Peacor, 1967). The square antiprisms, likewise, share edges to form chains along the *b* axis. The polyhedra about Na and octahedra about Mn share edges, thus forming continuous sheets of polyhedra parallel to (101). Adjoining sheets are linked by silicate chains of the wollastonite type. Bond lengths and angles are compared in Table 6a and Table 6b with those of pectolite (Prewitt, 1967). All bond lengths, angles, and atomic distances of pectolite and related structures to which reference is made later in the present paper were recalculated, based on atomic coordinates given by respective authors, using the same computational procedure we used for serandite. (There are several misprints in bond lengths given in the Trojer's (1968) parawollastonite paper.)

Distortion of silicate tetrahedra

Inspection of Tables 6a and 6b reveals that most values, including those of the Si–O bonds of serandite, are smaller than the corresponding values of pectolite. To study the effect of substituting Mn for Ca in the pectolite structure, we should first examine the difference in cell dimensions between pectolite and serandite (Table 2); the *a* and *c* lengths of serandite are shorter, compared to those of pectolite, by about 4 percent, whereas the *b* length is shorter only by 2 percent. The smaller amount of shrinkage in *b* may be explained in terms of the configuration of Si_3O_9 chains characteristic of pectolite–serandite series of structures. The silicate chains of the wollastonite type can be, in general, shortened or elongated parallel to their length by rotating each tetrahedron about its apical bond. However, in the particular case of pectolite, O(3) and O(4) of the silicate chain are unlike those in wollastonite, strongly bonded to Na, giving a very short O(3)–O(4) distance of 2.482 Å (Prewitt, 1967). That kind of rotation of tetrahedra which would give rise to a shortening of silicate chains would require a further decrease of this short O(3)–O(4) distance. Thus, shrinkage of octahedral bands which are flanked by silicate chains, appears to be hindered parallel to *b*, compared to other directions, by the configurational characteristics of silicate chains. Shrinkage of the silicate chains parallel to the *b* axis seems to be accomplished mainly by decreasing the Si–O bridge-

TABLE 4. Anisotropic thermal parameters of serandite ($\times 10^4$)

Atom	β_{11}	β_{22}	β_{33}	β_{12}	β_{13}	β_{23}
Mn(1)	31(1)	34(1)	29(1)	7(1)	5(1)	3(1)
Mn(2)	30(1)	38(1)	30(1)	11(1)	3(1)	-1(1)
Na	46(2)	96(3)	73(3)	12(2)	11(2)	-2(2)
Si(1)	27(1)	25(2)	29(2)	8(1)	-2(1)	-2(1)
Si(2)	27(1)	27(2)	25(2)	9(1)	1(1)	-2(1)
Si(3)	20(1)	34(2)	25(2)	6(1)	2(1)	1(1)
O(1)	30(4)	53(5)	54(5)	8(3)	15(3)	5(4)
O(2)	34(4)	53(4)	40(5)	6(3)	-2(3)	-2(4)
O(3)	65(4)	48(4)	44(4)	30(3)	10(3)	-3(4)
O(4)	62(4)	43(4)	44(4)	13(3)	15(3)	3(3)
O(5)	33(3)	60(5)	29(4)	7(3)	-2(3)	3(3)
O(6)	35(4)	56(5)	41(4)	15(3)	-4(3)	-7(4)
O(7)	35(4)	49(4)	48(4)	10(3)	0(3)	21(3)
O(8)	33(3)	47(4)	57(4)	16(3)	1(3)	-17(4)
O(9)	48(4)	33(4)	54(5)	10(3)	3(3)	4(3)

The expression used for the anisotropic thermal parameters was

$$\exp -(\beta_{11}h^2 + \beta_{22}k^2 + \beta_{33}l^2 + 2\beta_{12}hk + 2\beta_{13}hl + 2\beta_{23}kl)$$

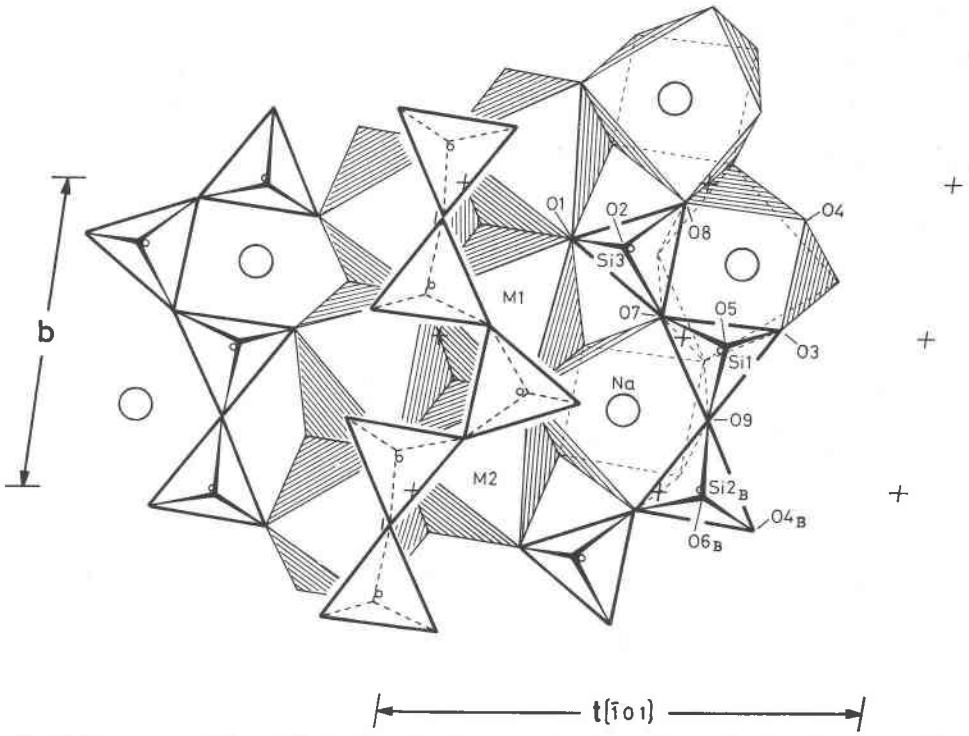

FIG. 1. The structure of serandite projected onto (101). Symmetry centers are indicated by crosses. The atoms $O4_B$, $O6_B$, and $Si2_B$ are respectively related, by translation *b*, to the atoms O4, O6, and Si2 (Table 3); the latter two are not shown.

bond lengths (Table 6a). The sum of the lengths of the bridge bonds, Si(1)–O(9), Si(2)–O(9), Si(3)–O(8), and Si(3)–O(7), which are parallel to or have large components parallel to *b*, is 6.536 Å; the corresponding sum for the pectolite structure is 6.620 Å. The difference of 0.084 Å is to be compared with a difference of 0.151 Å in the *b* length between pectolite and serandite. It is notable that the O(7)–O(8) edge of the Si(3) tetrahedron in the serandite structure is shorter than the corresponding edge in the pectolite structure by 0.06 Å. Since this edge is parallel to the *b* axis, this difference also contributes to the difference in the *b* length. In summary, the principal factor responsible for the shrinkage of silicate chains, upon substitution of Mn for Ca in the pectolite structure to give serandite, is the distortion of individual tetrahedra rather than a change in configuration of silicate chains.

In contrast to the bridge bonds, Si–O nonbridge bonds of serandite have lengths similar to those of pectolite (Table 7). The distortions of tetrahedra of the two structures are compared in Figure 2, in which each O–O edge of tetrahedra is plotted against the negative of the cosine of the O–Si–O angle subtended by the pair of oxygen atoms. The variation of entries in this diagram can be approximated, for constant bond lengths and small ranges of angles, by a straight line with a slope of 1.0. In the diagram we find that the sets of entries for serandite and pectolite respectively define lines having slopes of around 0.80 and 0.55. The difference in slope is mainly due to the difference in the bridge-bond lengths of these mineral species.

The shrinkage of bond lengths evidently originated with the substitution of Mn for Ca. Therefore, it seems that the difference in ionic radii, in chemistry of the atoms, *e.g.* electronegativity, or perhaps both are responsible for the shrinkage. Since Si–O(br) bridge bonds in general tend to be longer than Si–O(nbr) nonbridge bonds, the fact that the bridge bonds shrink upon substitution of Mn for Ca, and nonbridge bonds are nearly invariant implies a decreasing in the difference between Si–O(br) and Si–O(nbr) lengths. Since Mn is more electronegative than Ca, this situation is consistent with the finding (Brown and Gibbs, 1970) that the difference between Si–O(br) and Si–O(nbr) lengths decreases with increasing electronegativity of cations coordinated to the oxygen atoms. It does not explain the decreasing of Si–O(br) lengths. If angles at O(br)'s increased, the variation of Si–O(br) could be explained by d–$p\pi$ bonding theory (Cruickshank, 1961). On the contrary, the angles at O(br) decrease.

TABLE 6A. Comparison of bond lengths and angles of serandite and pectolite

Central atom			serandite		pectolite (Prewitt, 1967)	
			Bond length	Angle	Bond length	Angle
Si(1)	O(3)		1.627 Å		1.627 Å	
	O(5)		1.598		1.600	
	O(7)		1.642		1.649	
	O(9)		1.611		1.629	
	Average		1.620		1.626	
	O(3)	O(5)	2.728	115.6°	2.713	114.5°
		O(7)	2.635	107.4	2.623	106.4
		O(9)	2.571	105.1	2.609	106.6
	O(5)	O(7)	2.670	111.0	2.686	111.6
		O(9)	2.686	113.6	2.683	112.4
	O(7)	O(9)	2.548	103.1	2.596	104.8
	Average		2.640		2.652	
Si(2)	O(4)		1.607		1.605	
	O(6)		1.607		1.609	
	O(8)		1.649		1.655	
	O(9) B		1.613		1.642	
	Average		1.619		1.628	
	O(4)	O(6)	2.706	114.7	2.699	114.2
		O(8)	2.635	108.1	2.642	108.3
		O(9) B	2.610	108.3	2.647	109.2
	O(6)	O(8)	2.686	111.2	2.687	110.8
		O(9) B	2.666	111.7	2.671	110.5
	O(8)	O(9) B	2.535	102.0	2.585	103.3
	Average		2.640		2.655	
Si(3)	O(1)		1.597		1.592	
	O(2)		1.607		1.605	
	O(7)		1.661		1.673	
	O(8)		1.651		1.676	
	Average		1.629		1.637	
	O(1)	O(2)	2.721	116.3	2.711	116.0
		O(7)	2.658	109.3	2.669	109.7
		O(8)	2.675	110.9	2.673	109.8
	O(2)	O(7)	2.658	108.9	2.658	108.4
		O(8)	2.639	108.2	2.658	108.2
	O(7)	O(8)	2.583	102.5	2.642	104.2
	Average		2.656		2.652	
O(9)	Si(1)	Si(2)		146.2		147.8
O(7)	Si(1)	Si(3)		131.1		135.0
O(8)	Si(2)	Si(3)		135.5		136.4

Calculated standard errors are 0.003 Å for Si - O, and 0.004 Å for O - O, and 0.2° for bond angles.
B is a code indicator showing coordinates of atoms equivalent by b translation to the atoms at xyz given in Table 3.

TABLE 6B. Comparison of bond lengths of serandite and pectolite

Central atom		serandite	pectolite*
M(1)	O(1)	2.212 Å	2.323 Å
	O(2) i	2.265	2.336
	O(3) I	2.206	2.343
	O(5) A	2.350	2.438
	O(5) i	2.202	2.382
	O(6) A	2.282	2.385
	Average	2.253	2.368
M(2)	O(1) B′	2.173	2.313
	O(2) i	2.192	2.315
	O(4) I	2.153	2.321
	O(5) A	2.361	2.429
	O(6) i	2.241	2.409
	O(6) A B′	2.257	2.370
	Average	2.230	2.360
Na	O(2) i	2.242	2.312
	O(3) I	2.384	2.471
	O(4) I	2.461	2.497
	O(7)	2.487	2.537
	O(7) I	2.872	3.007
	O(8) I	2.710	2.977
	O(8) B′	2.468	2.534
	O(9)	2.257	2.305
	Average	2.485	2.580

Calculated standard errors are 0.003 Å.
A , B′, i , I are code indicators showing coordinates of atoms equivalent by space group operation to the atoms at xyz. Corresponding operations are :
A translation a
B′ translation -b
i inversion at 1/2, 1/2, 0
I inversion at 1/2, 1/2, 1/2.
Two code indicators in sequence imply an atom related to the one at xyz by successive application of the two symbolized operations.
* Prewitt (1967).

Hydrogen bonding

The separation between O(3) and O(4) is only 2.453(4) Å, which is even shorter than the corresponding distance of 2.482 Å in pectolite (Prewitt, 1967). The valence sums at O(3) and O(4), which were estimated following the procedure of Donnay and Allmann (1970), are 1.50 (*v.u.*) and 1.55 (*v.u.*), respectively. It thus appears that hydrogen bonding between O(3) and O(4) would occur, as suggested by Buerger (1956) and Prewitt (1967). In the final difference Fourier map, an ill-defined residual peak occurs in a region between O(3) and O(4), with its center approximately at $x = 0.14$, $y = 0.66$, $z = 0.55$. The position, which will be denoted *P*, is at a distance of 1.25 Å from both O(3) and O(4). The two lines O(3)–*P* and O(4)–*P* subtend an angle of 160° at *P* (Takéuchi and Kudoh, 1972), the result being nearly the same as that reported by Prewitt (1967) for pectolite. Since the peak is broad and not significantly above the background, the hydrogen location is not accurately known.

If we locate the hydrogen atom at position *P*, a very distorted tetrahedron is constructed of the hydrogen, Mn, Na, and Si around each of O(3) and O(4). The Na–O(3)–H and Na–O(4)–H angles are, for example, only 71° and 68°, respectively. It is to be noted that the Na atom is shared by the two tetrahedra (Fig. 3a), the distance between Na and H being

TABLE 7. Mean Si-O lengths of serandite and pectolite

	serandite	pectolite*
Nonbridge bond	1.607 Å	1.606 Å
Bridge bond	1.638	1.654
Angle at O(br)	137.6°	139.7°

* Prewitt (1967).

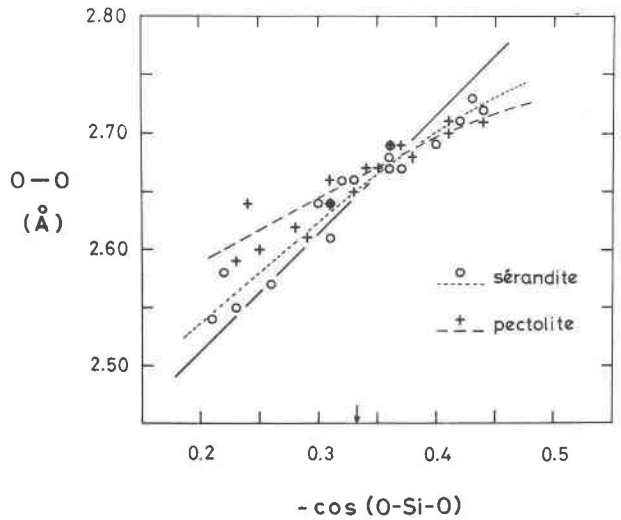

FIG. 2. Variations of O–O edge lengths with the negative of the cosine of O–Si–O angles. The minus cosine value for the tetrahedral angle is indicated by an arrow. The straight line represents the variations for the case of constant Si–O length 1.623 Å which corresponds to the average Si–O length in serandite.

only 2.30 Å. This situation arises from the fact that the line segment O(3)–O(4) is one of the edges of the polyhedron about Na, and that the hydrogen atom is nearly on this line.

Because of such a novel feature of the hydrogen bonding, a search was made for other anion neighbours of O(3) and O(4). We found that O(3) has, at a distance 2.835(4) Å, another near oxygen neighbour, O(3)′, which is related to O(3) by an inversion operation. The oxygen O(3)′ is at a distance of 3.147(4) Å from O(4). It is thus possible to postulate an alternate model of hydrogen bonding with 1/2 hydrogen atoms attached to O(4) and O(3), each O–H dipole directed to O(3)′ (Fig. 3b). In this case, there would probably be formed a weak hydrogen-bond between O(3) and O(3)′. In this model, however, the hydrogen atoms are slightly closer to Si atoms than in the first model. The above argument seems to indicate that the formation of nearly symmetrical hydrogen bonding between O(3) and O(4) is more likely.

The infrared spectra of serandite, like those of pectolite (Ryall and Threadgold, 1966), show a strong absorption band at 1350 cm^{-1} which according to Ryall and Threadgold (1966) is due to O–H bending mode. In addition to this band, our spectra show a significant band at 3420 cm^{-1}. Since the absorption bands at this frequency may be assigned to the O–H stretching mode characteristic of weak hydrogen-bonded systems, the result is in conflict with the above conclusion drawn from structural considerations. To fully establish the existence of the nearly symmetrical hydrogen bonding, more detailed infrared study using single crystals is desirable.

Pseudosymmetry and polytypism

The structure of serandite has, like that of pectolite, a marked $P2_1/m$ pseudosymmetry, with b as unique axis; the maximum deviation from that symmetry is 0.16 Å in atomic coordinates and averages 0.08 Å. It is then possible, in general, to derive, as in the case of wollastonite (Takéuchi, 1972b), various polytypic variants from the serandite structure by

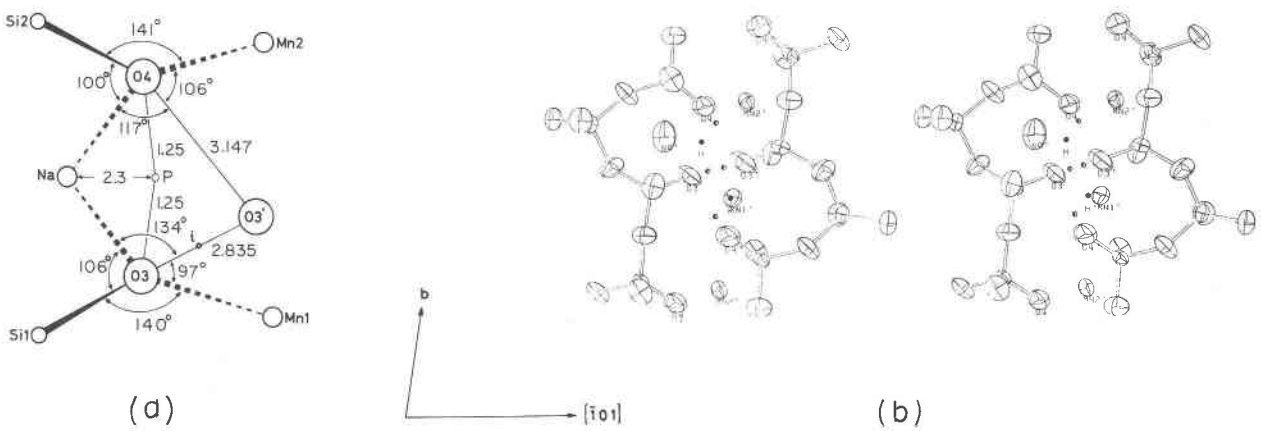

FIG. 3. (a) Neighbors of O(3) and O(4). The position P, and the center of symmetry i between O(3)′ and O(3) are indicated. Some important angles that are not shown in the diagram are: Si(2)–O(4)–P = 115.7°, Si(2)–O(4)–O(3)′ = 104.9°, Si(1)–P = 118°, Si(1)–O(3)–O(3)′ = 95.6°. (b) Stereographic drawing a pair of silicate chains related to each other by inversion operation. Solid circles indicate hydrogen locations corresponding to P, and half-filled circles are those of an alternate model discussed in the text. The computer program ORTEP (Johnson, 1965) was used to provide this figure.

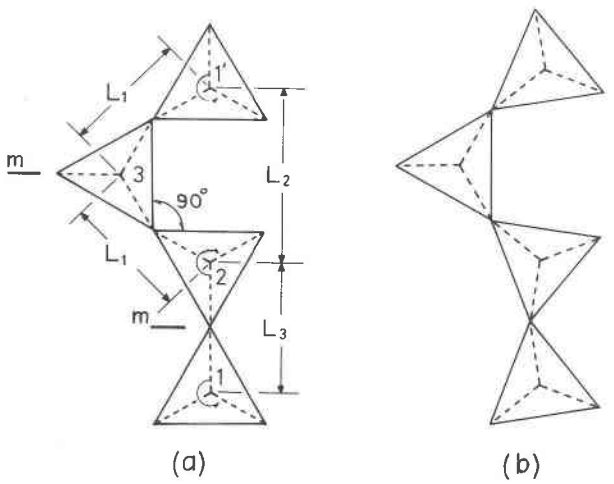

FIG. 4. Links of regular tetrahedra showing an idealized Si_3O_9 chain (a). Characteristic distances between apical oxygens are shown. For Si–O = 1.61 Å, L_1 = 2.96 Å, L_2 = 4.18 Å, L_3 = 3.06 Å. The chain has mirror planes as indicated. Rotations of tetrahedra 1, 2, and 1 1 in the directions indicated give rise to a configuration shown in (b).

generating periodic displacements, by $b/2$, of silicate chains (and chains of Na polyhedra), octahedral bands being left unshifted. The displacement by $b/2$ of silicate chains is permissible primarily because of the strong pseudotranslation, $b/2$, of octahedral bands. However if Ca and Mn are ordered, as in the present structure, the pseudotranslation of the octahedral bands is in fact removed. Therefore, polytypism of the serandite–pectolite series would not occur in the intermediate phases in which the ordering of octahedral cations is expected, but would be limited only to pure end members. As a matter of fact, Müller (personal communication) has found, based on an electron microscopic study, a monoclinic variant of a pectolite end member but no variant in the serandite crystals which we used for the present study.

The variation in configuration of Si_3O_9 chains

Our structural analysis of serandite has brought out evidence that Ca is preferably located in the $M(1)$ position. To interpret this mode of cation order in comparison with that in bustamite (Peacor and Buerger, 1962), we found it desirable to study the general relations between the configuration of octahedral bands and those of adjacent silicate chains. In the structures under consideration, the apical oxygens of each adjacent pair of tetrahedra in a given Si_3O_9 chain are attached to the same octahedron; the distance between the oxygen atoms define an edge length of the octahedron. Consequently, the Si–O–Si bridge angle varies, in general, depending upon the edge length, *i.e.* the size of the octahedral cations.

The general configuration of the Si_3O_9 chains may be examined starting with an idealized chain (Fig. 4), which is similar to that in serandite (and pectolite). As can be observed in this figure, the relative lengths of the octahedral edges are: $L_2 > L_3 > L_1$. If the tetrahedra are buckled, as occurs in serandite and pectolite, L_3 is lengthened, while L_2 shortened. If tetrahedra 1 and 2 are tilted by 15°, L_3 becomes longer than L_2. On the other hand, if tetrahedra 1 and 2 are rotated by 10° in the directions shown in Figure 4a, we obtain a configuration (Fig. 4b) similar to that of wollastonite chains. Since a rotation of that amount does not change the lengths L_1 and L_3 significantly, the above argument suggests that L_1 will remain the shortest edge. The lengths of octahedral edges formed by silicate-chain apical oxygens, together with Si–O bond lengths and angles at O(br), are given in Tables 8 and 9 for each of the wollastonite group minerals. Note that the variations in edge lengths are in agreement with the above results based on geometrical considerations.

Ordering of cations

The preference of Ca for the $M(1)$ site in serandite (Fig. 5a) can now be explained bearing the above arguments in mind. Since the edge, O(5)–O(6), which belongs to the $M(1)$ octahedron, tends to be longer, as argued above, the $M(1)$ octahedron is better able to accommodate larger cations, with a minimum of distortion of the attached silicate chain. It is thus expected that in the pectolite–serandite series, the larger Ca will concentrate, as found in the present structure, at the $M(1)$ site, while Mn will prefer the $M(2)$ site.

TABLE 8. Characteristic distances between apical oxygens of silicate tetrahedra

	Characteristic distances			
	L_3	L_1	L_2	$(L_3-L_1)/L_3$
serandite	3.413 Å	3.136 Å	3.477 Å	8.1 %
pectolite (1)	3.444	3.291	3.597	4.4
wollastonite (2)	3.847	3.408	3.473	11.4
parawollastonite (3)	3.836	3.402	3.484	11.3
bustamite (4)	3.862	3.250	3.297	15.9
$Wo_{50}Fs_{50}$* (5)	3.852	3.229	3.260	16.4

(1) Prewitt (1967), (2) Prewitt and Buerger (1963), (3) Trojer (1968), (4) Peacor and Buerger (1962), (5) Rapoport and Burnham (1973).
* Wo=wollastonite component, Fs=ferrosilite component.

TABLE 9. Angles at O(br) and mean bridge-bond lengths

	T_1-O-T_2*		T_2-O-T_3 and T_3-O-T_1,	
	Angle	Bond length	Angle**	Bond length**
serandite	146°	1.612 Å	133°	1.651 Å
pectolite (1)	148	1.636	136	1.666
wollastonite (2)	149	1.642	140	1.666
parawollastonite (3)	149	1.636	140	1.654
bustamite (4)	161	1.615	136	1.659
$Wo_{50}Fs_{50}$ (5)	163	1.614	136	1.647
Average	153	1.626	136	1.657

* See Fig. 4 for identification of angles and bond lengths.
** Average of two. (1) Prewitt (1967), (2) Prewitt and Buerger (1963), (3) Trojer (1968), (4) Peacor and Buerger (1962), (5) Rapoport and Burnham (1973).

It appears that the above scheme of cation ordering is not only applicable to the pectolite–serandite series but to pyroxenoid structures in general. In the structure of the Li end-member of nambulite, $LiMn_{3.66}Mg_{0.34}Si_5O_{14}(OH)$, (Murakami *et al.*, in preparation), smaller Mg atoms preferably substitute for Mn atoms in octahedra corresponding to $M(2)$ of Figure 5a.

In the wollastonite structure (Prewitt and Buerger, 1963), the silicate chain occurs above the face of an octahedron (octahedron A of Fig. 5b). All three corners of this face are formed by the apical oxygens of the chain. On the opposite face of this octahedron, only the edge O(3)–O(4) is formed by the apical oxygens of another silicate chain. In the wollastonite structure the tetrahedral chains are considerably tilted, and as a result the upper face of octahedron A is contracted while the opposite face is widened; the three O–O edges of the upper face have a mean value of 3.429 Å, while those of the opposite face average 3.796 Å.

If the silicate chain connected to the lower side of octahedron A were displaced by $b/2$, both sides of the octahedron would have all three corners formed by apical oxygens of tetrahedral chains. As a result, the octahedron would have both faces compressed, a condition which is more favorable for accommodation of cations smaller than Ca. This configuration occurs in the structure of bustamite (Peacor and Buerger, 1962) (Fig. 5c); the octahedron corresponding to A is fully occupied by Mn (the octahedral site was denoted as $M(3)$ by Rapoport and Burnham (1973), and as Mn_2 by Peacor and Buerger (1962)).

The Mn cations in the bustamite structure are located in both the $M(3)$ and the $M(1)$ sites (Fig. 5c). Since the size of the $M(1)$ octahedron may be adjusted to accommodate Ca by slight distortions of silicate chains and possibly of tetrahedra, it appears

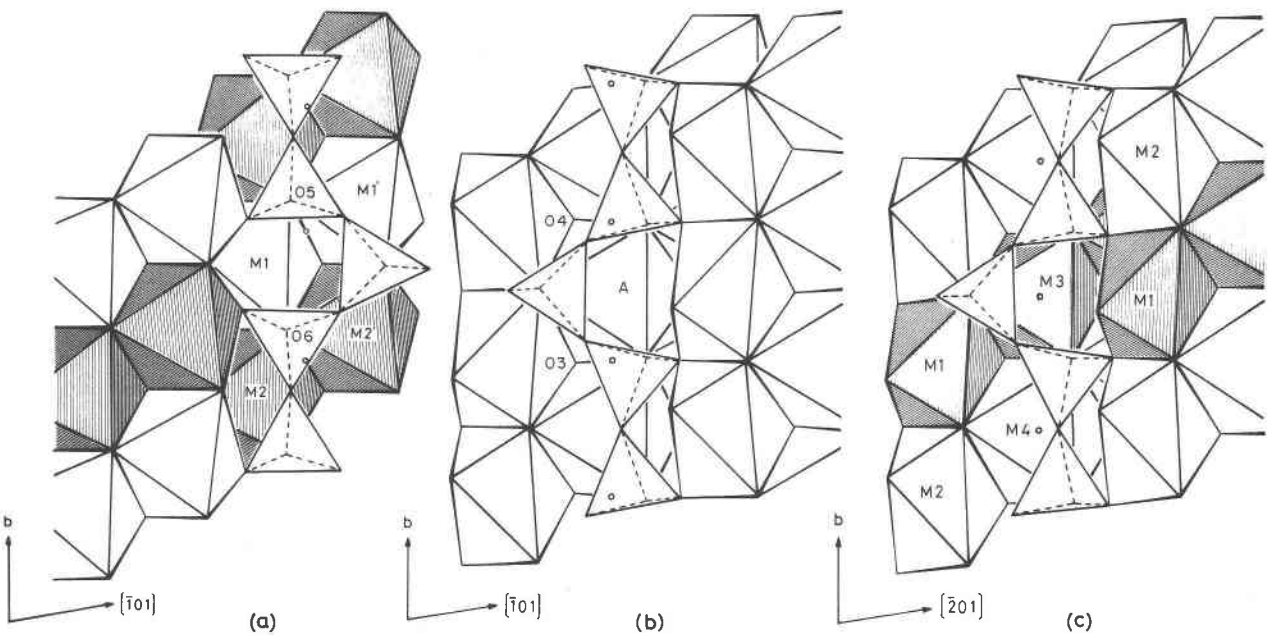

FIG. 5. Relations between cation ordering in octahedral bands and locations of Si_3O_9 chains attached to the bands. (a) *Serandite*. The octahedra fully occupied by Mn are shaded. A set of centers of symmetry located on octahedral edges are indicated by small circles. (b) *Wollastonite*. A set of centers of symmetry on octahedral edges are indicated by small circles. (c) *Bustamite*. The octahedra containing Mn are shaded, others are occupied by Ca. A set of centers of symmetry in octahedra are indicated by small circles. In each figure, only part of the upper octahedral bands is shown.

that the bustamite type structure may occur for the compositions from $Ca_3Mn_3(Si_3O_9)_2$ to $Ca_5Mn(Si_3O_9)_2$. For the latter composition Mn cations occur only in the Mn(3) site, with other octahedra occupied by Ca cations. Bustamite crystals whose Mn content is only slightly higher than that of the above Mn-poor composition have been reported (Mason, 1975). Likewise, an occurrence has been reported of iron analogs, $Wo_{79}Fs_{21}$ (Rapoport and Burnham, 1973) and $Wo_{81}Fs_{19}$ (Matsueda, 1973; Shimazaki and Yamanaka, 1973). Structure analysis of $Wo_{79}Fs_{21}$ (Rapoport and Burnham, 1973) revealed that Fe cations concentrated over the $M(3)$ and $M(4)$ sites. In addition, the structure of $Wo_{81}Fs_{19}$ determined by one of the present authors (T. Y.) has revealed that Fe cations are perfectly ordered at the $M(3)$ site, supporting our scheme of cation distribution.

Acknowledgments

We wish to thank Professor Takeo Watanabe for kindly placing his serandite specimens at our disposal and for continued encouragement, and Dr. Wolfgang F. Müller, Universität Frankfurt am Main, for carrying out an electron-microscopic study of serandite using our specimens and for permission to quote his results in this paper. Computations were carried out on HITAC 8700/8800 at the Computer Center of the University of Tokyo.

References

BROWN, G. E., AND G. V. GIBBS (1970) Stereochemistry and ordering in the tetrahedral portion of silicates. *Am. Mineral.*, **55,** 1587–1607.

BUERGER, M. J. (1956) The determination of the crystal structure of pectolite, $Ca_2NaHSi_3O_9$. *Z. Kristallogr.* **108,** 248–262.

BUSING, W. R., K. O. MARTIN, AND H. A. LEVY (1962) ORFLS, a FORTRAN crystallographic least squares program, ORNL-TM 305, Oak Ridge National Laboratory, Oak Ridge, Tennessee.

CRUICKSHANK, D. W. J. (1961) The role of 3-*d* orbitals in π-bonds between (a) silicon, phosphorus, sulfur, or chlorine and (b) oxygen or nitrogen. *J Chem. Soc.* 5486–5504.

——— (1965) Errors in least-squares methods. In, J. S. Rollet, Ed., *Computing methods in crystallography.* Pergamon Press, New York.

DONNAY, G., AND R. ALLMANN (1970) How to recognize O^{-2}, OH^- and H_2O in crystal structures determined by X-rays. *Am. Mineral.* **55,** 1003–1015.

FINGER, L. W. (1969) Determination of cation distributions by least-squares refinement of single-crystal x-ray data. *Carnegie Inst. Wash. Year Book,* **67,** 216–217.

FREED, R. L., AND D. R. PEACOR (1967) Refinement of the crystal structure of johannsenite. *Am. Mineral.* **52,** 709–720.

HAMILTON, W. C. (1959) On the isotropic temperature factor equivalent to a given anisotropic temperature factor. *Acta Crystallogr.* **12,** 609–610.

HOWELLS, E. R., D. C. PHILLIPS, AND D. ROGERS (1950) The probability distribution of x-ray intensities. II. Experimental investigation and the x-ray detection of centres of symmetry. *Acta Crystallogr.* **3,** 210–214.

JOHNSON, C. K. (1965) ORTEP:FORTRAN thermal ellipsoid plot program for crystal structure illustrations. Report ORNL-3794, Oak Ridge National Laboratory, Oak Ridge, Tennessee.

MASON, B. (1975) Compositional limits of wollastonite and bustamite. *Am. Mineral.* **60,** 209–212.

MATSUEDA, H. (1973) Iron-wollastonite from Sampo mine showing properties distinct from those of wollastonite. *Mineral. J. (Japan),* **7,** 180–201.

PEACOR, D. R., AND M. J. BUERGER (1962) Determination and refinement of the crystal structure of bustamite, $CaMnSi_2O_6$. *Z. Kristallogr.* **117,** 335–343.

———, AND C. T. PREWITT (1963) Comparison of the crystal structures of wollastonite and bustamite. *Am. Mineral.* **48,** 588–596.

PREWITT, C. T. (1967) Refinement of the structure of pectolite, $Ca_2NaHSi_3O_9$. *Z. Kristallogr.* **125,** 298–316.

———, AND M. J. BUERGER (1963) Comparison of the crystal structures of wollastonite and pectolite. *Mineral. Soc. Am. Spec. Paper* **1,** 293–302.

———, AND D. R., PEACOR (1964) Crystal chemistry of the pyroxenes and pyroxenoids. *Am. Mineral.* **49,** 1527–1542.

RAPOPORT, P. A., AND C. W. BURNHAM (1973) Ferrobustamite: The crystal structure of two Ca,Fe bustamite-type pyroxenoids. *Z. Kristallogr.* **138,** 419–438.

RYALL, W. R., AND M. THREADGOLD (1966) Evidence for $[(SiO_3)_5]_\infty$ type chain in inesite as shown by x-ray and infrared absorption studies. *Am. Mineral.* **51,** 754–761.

SCHALLER, W. T. (1955) The pectolite–schizolite–serandite series. *Am. Mineral.* **40,** 1022–1031.

SIHMAZAKI, H., AND T. YAMANAKA (1973) Iron-wollastonite from skarns and its stability relation in the $CaSiO_3$–$CaFeSi_2O_6$ join. *Geochem. J. (Japan),* **7,** 67–79.

TAKÉUCKI, Y. (1972a) The investigation of superstructures by means of partial Patterson functions. *Z. Kristallogr.* **135,** 120–136.

——— (1972b) Polymorphic or polytypic changes in biotites, pyroxenes and wollastonite (in Japanese). *J. Mineral. Soc. Japan,* **10,** *Spec. Paper* **2,** 87–99.

———, AND Y. KUDOH (1972) Valence balance of hydrogen-bonded systems in certain rock-forming silicates. *Acta Crystallogr.* **A28 Suppl.,** 66–67.

———, Y. KUDOH AND N. HAGA (1973) The interpretation of partial Patterson functions and its application to structure analyses of sérandite $NaMn_2HSi_3O_9$ and banalsite $BaNa_2Al_4Si_4O_{16}$. *Z. Kristallogr.* **138,** 313–336.

TROJER, F. J. (1968) The crystal structure of parawollastonite. *Z. Kristallogr.* **127,** 291–308.

Manuscript received, July 28, 1975; accepted for publication, November 10, 1975.